Title

Response of plasmodesmata formation in leaves of C_4 grasses to growth irradiance

Authors

Florence R. Danila[1,2*], William Paul Quick[2,3,5], Rosemary G. White[4], Susanne von Caemmerer[1,2], Robert T. Furbank[1,2,4]

Contact information

[1]Research School of Biology, Australian National University, Canberra Australian Capital Territory 2601, Australia. [2]ARC Centre of Excellence for Translational Photosynthesis, Australian National University, Canberra Australian Capital Territory 2601, Australia. [3]International Rice Research Institute, Los Baños, Laguna 4030, Philippines. [4]CSIRO Agriculture and Food, Canberra Australian Capital Territory 2601, Australia. [5]University of Sheffield, Sheffield, United Kingdom.

*To whom correspondence should be addressed. E-mail: florence.danila@anu.edu.au

Funding

This research was funded by the Australian Government through the Australian Research Council Centre of Excellence for Translational Photosynthesis (CE1401000015).

Abstract

Rapid metabolite diffusion across the mesophyll (M) and bundle sheath (BS) cell interface in C_4 leaves is a key requirement for C_4 photosynthesis and occurs via plasmodesmata (PD). Here, we investigated how growth irradiance affects PD density between the M and BS cells and between M cells in two C_4 species using our PD quantification method, which combines three-dimensional laser confocal

fluorescence microscopy and scanning electron microscopy. The response of leaf anatomy and physiology of the NADP-ME species, *Setaria viridis* and *Zea mays* to growth under different irradiances, low light (100 µmol m^{-2} s^{-1}) and high light (1000 µmol m^{-2} s^{-1}), was observed both at seedling (two weeks after germination) and established (seven weeks after germination) growth stages. We found that the effect of growth irradiance on C_4 leaf PD density depended on plant age and species. The high light treatment resulted in two to four-fold greater PD density per unit leaf area than at low light, due to greater area of PD clusters, and to a lesser extent to greater PD size, in plants grown at high light. These results along with our finding that the effect of light on M-BS PD density in these experiments was not tightly linked to photosynthetic capacity suggest a complex mechanism underlying the dynamic response of C_4 leaf PD formation to growth irradiance.

Keywords

Plasmodesmata density, growth irradiance, *Setaria viridis*, *Zea mays*, plant age, photosynthetic capacity

Abbreviations

NADP-ME, nicotinamide adenine dinucleotide phosphate-malic enzyme; PCK, phosphoenolpyruvate carboxykinase

Acknowledgements

We thank the ANU Centre for Advanced Microscopy (CAM), Australian Microscopy and Microanalysis Research Facility (AMMRF), and CSIRO Black Mountain MicroImaging Centre (BMIC) for providing support and technical assistance. This research was funded by the Australian Government through the Australian Research Council Centre of Excellence for Translational Photosynthesis (CE1401000015). F.R.D is also financially supported by the Lee Rice Foundation scholarship through the International Rice Research Institute, Philippines.

Introduction

High photosynthetic efficiency in C_4 plants is attributed to the ability to concentrate carbon dioxide at the site of rubisco (ribulose-1,5-biphosphate carboxylase/oxygenase), consequently diminishing photorespiration (Hatch, 1987). In a C_4 leaf, fixation of atmospheric CO_2 and photosynthetic carbon reduction are spatially separated into two anatomically and biochemically distinct cells (Kranz anatomy); these are the mesophyll (M) and bundle sheath (BS) cells, respectively (Hatch and Osmond, 1976). The CO_2-tight anatomy of BS cells and high affinity of carbonic anhydrase and phosphoenolpyruvate carboxylase (PEPC) to CO_2 and bicarbonate respectively, contribute to the elevation of CO_2 around the active site of Rubisco to levels up to ten fold ambient CO_2 concentrations in the mesophyll (Furbank et al., 1990; Hatch, 1987; von Caemmerer and Furbank, 2003). While the efficiency of the CO_2 concentrating mechanism is reliant on minimising diffusion of CO_2 out of the BS cells, rapid metabolite exchange between M and BS during C_4 photosynthesis is required to support photosynthetic flux of C_4 acids to the BS cells and for C_3 products to return to the mesophyll to regenerate PEP. Given that the M-BS cell interface is characterised by cell walls which are heavily thickened and often suberised, metabolites must pass symplastically across this barrier, via diffusion through plasmodesmata (PD) (Hatch and Osmond, 1976).

PD are cytoplasmic conduits that traverse plant cell walls to enable intercellular continuity. Evidence for the existence of PD in plants was published more than a hundred years ago (Tangl, 1879) but a comprehensive understanding of their role in developmental, intercellular transport and signalling processes as well as their molecular anatomy and genetic networks controlling their function still remains to be realised (Lu et al., 2018). The main challenge underlying PD research has been their minute size and difficulty in viable isolation. For a long time, transmission electron microscopy-based methods have been used to quantify the intercellular PD connections between plant cells using arduous serial sectioning and visual counting of PD (Botha, 1992; Gunning, 1978; Seagull, 1983). This has limited both data accuracy due to the 3-D nature of cell interfaces and patchy, non-random distribution of PD at those interfaces, and statistical robustness due to insufficient sampling coverage. The application of 3-D imaging of intact plant tissue to this problem

(Danila et al., 2016) has avoided many of these limitations and provided not only more accurate PD density measurements in leaves but also the first comprehensive PD density survey in monocot species (Danila et al., 2018). In the latter study, C_4 grasses were found to have up to 12 times more PD connecting photosynthetic cells compared to the C_3 species (Danila et al., 2018).

The CO_2 concentrating mechanism of C_4 photosynthesis requires at least 2 additional ATP per CO_2 fixed compared to C_3 photosynthesis (Furbank et al., 1990) thus, C_4 plants suffer an energetic penalty under some environmental conditions. Indeed, in natural ecosystems C_4 plants are typically found in high light environments under higher ambient temperatures where the benefits of the CO_2 concentrating mechanism outweigh the costs (Sage and Pearcy, 2000). Nevertheless, in most field situations where C_4 crops and grasses form thick canopies, a substantial proportion of the vegetative part of the plant may experience shade or natural low light. Under such unfavourable conditions, C_4 leaves can undergo both biochemical and anatomical changes as part of their acclimation response (Pengelly et al., 2010; Sonawane et al., 2018; Tazoe et al., 2006). Responses of C_4 plants, however, appear to differ depending on the decarboxylation subtype (NADP-ME, NAD-ME, or PCK), whether the plants are monocots or dicots, or even between species (Tazoe et al., 2006). Photosynthetic efficiency may also be compromised in low light-grown C_4 plants which have been reported to show lower CO_2 assimilation rates compared to high light-grown plants (Sharwood et al., 2014; Sonawane et al., 2018).

Despite the importance of PD in facilitating transport between M and BS in C_4 plants, there is only one report of the effects of different growth irradiance on PD density in C_4 grass leaves (Sowiński et al., 2007). This study concluded that there was a proportional increase in M-BS PD density with increasing light intensity across all subtypes. However, the transmission electron microscopy technique described above was used, giving a restricted view of PD distribution over this 3D cell-cell interface, hence it is not clear how these changes were achieved. In most tissues, including leaves, PD occur in clusters, one unit of which is termed a pit field. Therefore, the use of the Gunning constant (Gunning, 1978) to calculate PD density in leaves (which requires random distribution of PD on the cell interface, not

clustering in pit fields) may not be appropriate for these calculations when PD are so highly clustered in pit fields (Sowinski et al 2007).

In this study, two NADP-ME C_4 grasses, *Setaria viridis* and *Zea mays,* were grown under different light intensities: low light (100 µmol m^{-2} s^{-1}) and high light (1000 µmol m^{-2} s^{-1}). The use of *Z. mays* allows comparison with previous studies while the information generated for *S. viridis* adds to the existing knowledge about this new C_4 model species with a relatively small sequenced and publicly available genome (Brutnell et al., 2010; Li and Brutnell, 2011). The response of PD frequency between leaf cells to growth under the two different light environments was evaluated by quantifying the PD density between M and BS on the youngest fully expanded leaf at two time points in plant development: two weeks and seven weeks after germination. Implementation of our PD quantification method (Danila et al., 2016) provided detail on how PD density changed expressed both in terms of PD frequency and pit field area. Concurrent with anatomical measurements, the response of photosynthetic assimilation to light intensity was measured and a range of other leaf physiological and anatomical parameters were characterised.

Materials and methods

Plant material and growth conditions

Seeds of *Setaria viridis* cultivar A10 and *Zea mays* cultivar B73 were germinated in a growth cabinet (High Resolution Plant Phenomics Centre, CSIRO Black Mountain, Canberra, Australia) under two light conditions, 100 µmol m^{-2} s^{-1} (low light) and 1000 µmol m^{-2} s^{-1} (high light). Cabinets were maintained at 28ºC day/22ºC night temperatures, 60% relative humidity, 16-hour light/8-hour dark, and ambient CO_2 concentration. Plants were supplied with Osmocote (Scotts Australia) and watered regularly. Physiological and anatomical parameters were measured on the youngest fully expanded leaf at two developmental stages: two weeks and seven weeks after germination.

Physiological measurements

Gas exchange was measured using a LI-6400 equipped with a blue-red light-emitting diode (LED) light source (LI-COR, Inc., Australia) applied to the middle portion of the youngest fully expanded leaf from three independent plants per species. Leaves were initially equilibrated for 30 minutes in a standard environment of 380 µmol mol^{-1} CO_2 set in sample cell, 25^oC leaf temperature, flow rate of 500 µmol s^{-1}, and an irradiance of 2000 µ$molm^{-2}$ s^{-1}. Light response curves were generated by imposing a stepwise decrease in irradiance (2000, 1500, 1000, 800, 600, 400, 200, 100, 0 µmol m^{-2} s^{-1}), each step lasting for 5 minutes while maintaining temperature and CO_2 conditions. Immediately following gas exchange measurements, two sets of 0.6 cm^2 leaf discs were collected from the same leaf, one set was snap-frozen in liquid nitrogen and the other set was oven-dried at 60^oC for 48 h. Chlorophyll was extracted from the frozen leaf discs using 80% acetone in mortar and pestle. Chlorophyll *a* and *b* proportions of the extract were calculated according to (Porra et al., 1989) using values obtained from Cary® 50 Bio UV-Visible Spectrophotometer (Varian, Inc.) at 663.6, 646.6, and 750 nm wavelengths. Using dried leaf discs, leaf mass per area was obtained by dividing dry weight by leaf area while total leaf nitrogen content was determined on the ground leaf tissue using a CN analyser (LECO TruSpec; LECO Corp., MI, USA).

Anatomical measurements

All leaf tissue preparations for light microscopy, transmission electron microscopy (TEM), scanning electron microscopy (SEM), and 3-D immunolocalisation confocal microscopy were as described by (Danila et al., 2016). Tissues were collected from the middle portion of the same leaf used for physiological measurement. Leaf tissues were fixed and processed accordingly. For 3-D immunolocalisation confocal microscopy, leaf tissue was fixed and cleared according to (Danila et al., 2016), hybridised with β-1,3-glucan (callose) antibody, followed by Alexa488-tagged secondary antibody, and post-stained with calcofluor white to visualise cell walls (Danila et al., 2016). Transverse sections of resin embedded leaves were imaged for light microscopy under 10X and 40X objectives using a Nikon Eclipse 50i upright microscope (Nikon Instruments). For TEM, ultrathin sections were examined using a Hitachi HA7100 transmission electron microscope (Hitachi High Technologies

America) at 75 kV. SEM was performed using a Zeiss Ultra Plus field emission scanning electron microscope at 3 kV.

To quantify pit field distribution, z-stacks from two leaf tissues per plant were obtained using a Leica SP8 multiphoton confocal microscope (Leica Microsystems). PD density was quantified using the method described in (Danila et al., 2016). PD area and pit field area were measured using SEM images. M-BS PD area per leaf area was calculated according to (Danila et al., 2018). Vein circumference, interveinal distance, and leaf thickness of 10 to 20 individual minor veins were measured from light micrographs of transverse leaf sections. Values for M and BS cell wall thickness, M and BS chloroplast size, M and BS starch granule per chloroplast, M and BS starch granule size, M grana width, and BS chloroplast content were obtained from TEM measurements of transverse leaf sections. Average number of corresponding structures measured was specified in Tables 2 and 3. Because chloroplasts and starch granules were not circular, the measurements performed here were used only for approximate comparison given that all samples were treated the same way. BS chloroplast content was calculated as the proportion of BS cell area taken up by the chloroplasts. BS surface area per unit leaf area (S_b) (n=7 or more) was calculated using the equation described previously (Pengelly et al., 2010). A Wacom Cintiq graphics tablet (Wacom Technology Corporation, Vancouver, WA, USA) together with ImageJ software (National Institutes of Health, Bethesda, MD, USA) were used for all anatomical measurements.

Statistical analysis

Group sizes were equal overall for all response variables. The relationship between various response variables and the main effect (growth irradiance and plant age) and their interactions were obtained using two-way ANOVA (OriginPro 9.1, OriginLab Corporation). Means comparisons were performed using post-hoc Tukey test at 0.05 significance level.

Results

CO_2 assimilation rate and leaf chemistry

In *S. viridis*, light response curves of CO_2 assimilation showed that plants grown under low light conditions had reduced photosynthetic performance when compared to their high light-grown counterparts regardless of plant age (Fig. 1A; Table 1). Similarly, low light-grown *Z. mays* had lower CO_2 assimilation rates than high light-grown plants but there was a significant plant age and growth irradiance x plant age effect on CO_2 assimilation rate (Fig. 1B; Table 1). Low CO_2 assimilation rate in low light-grown plants was particularly evident when plants were measured at high irradiance (Fig. 1C, D). In both *S. viridis* and *Z. mays*, plants grown at low irradiance had 30-50% less leaf mass per area compared to high light-grown plants and across development, high light-grown plants showed a greater leaf mass per area increase over time (Figs. 2A, 3A; Table 1). Significant effect of growth irradiance was also reflected in both total leaf N content (Figs. 2B, 3B; Table 1) and chlorophyll content per leaf area (Figs. 2C, 3C; Table 1) of *S. viridis* and *Z. mays*, where low light-grown plants had lower values.

Leaf anatomy

There was a significant plant age and growth irradiance x plant age effect on BS chloroplast content and chloroplast size in *S. viridis* (Fig. 2D; Tables 1, 2). Specifically, seven week-old *S. viridis* grown under low light had lower BS chloroplast content (Fig. 2D) but bigger chloroplasts (Table 2) compared to the high light-grown plants. In *Z. mays*, growth irradiance had a significant effect on both BS chloroplast content and chloroplast size (Table 1) where low light-grown plants have lower BS chloroplast content (Fig. 3D; Table 1) and smaller chloroplasts (Tables 1, 3) than the high light-grown plants. For both species, smaller leaf veins (Figs. 2E, 3E; Table 1), shorter interveinal distance (Figs. 2F, 3F; Table 1), and thinner leaves (Figs. 2G, 4A-D, 3G, 5A-D; Table 1) were observed in plants grown under low light indicative of reduced investment in photosynthetic machinery per unit leaf area, which is also seen in the strong correlation between photosynthetic rate and leaf N content (Supplementary Fig. 1). Transmission electron micrographs also revealed thinner cell walls in both BS (Figs. 2H, 3H; Table 1) and M (Figs. 2I, 3I; Table 1) cells in low light plants. There were also more and larger starch granules in both the M and BS chloroplasts in leaves of low light plants compared to the high light plants

(Figs. 4E-L, 5E-L; Tables 1, 2, 3). Grana width was significantly wider in BS chloroplasts of two week-old high light *S. viridis* and M chloroplast of seven week-old low light *S. viridis*, while there was no significant difference observed in grana development between low light and high light-grown *Z. mays* (Figs. 4I-L, 5I-L; Tables 1, 2, 3).

Plasmodesmata connections between mesophyll and bundle sheath

Overall, there was significant growth irradiance, plant age, and interaction effect on M-BS PD parameters in both *S. viridis* and *Z. mays* (Table 1). M-BS PD area per unit leaf area in *S. viridis* leaves was four-fold greater in high light plants compared to low light plants in seven-week old plants while in younger plants, low light plants had greater M-BS PD area per unit leaf area (Fig. 6A; Table 1). In addition to lower BS surface area per unit leaf area (S_b) (Fig. 6B), the reduction in M-BS PD area per unit leaf area in seven-week old low light-grown *S. viridis* resulted from smaller pit fields (Figs. 4M-P, 6C) populated by smaller PD (Fig. 6E), lower pit field area per unit cell interface area (Figs. 4Q-T, 6I) and lower number of PD per unit cell interface area (Fig. 6K). Meanwhile, bigger PD (Fig. 6E), greater pit field area per unit cell interface area (Fig. 6I) and more PD per unit cell interface area (Fig. 6K) resulted in a greater M-BS PD area per unit leaf area in two week-old low light *S. viridis*.

In two week-old *Z. mays*, high light plants had two-fold greater M-BS PD area per unit leaf area compared to the low light plants while in older plants, this gap was greatly reduced (Fig. 7A; Table 1). The smaller M-BS PD area per unit leaf area discrepancy between low light and high light plants in older *Z. mays* was a result of significantly smaller pit field size (Fig. 7C) and PD area (Fig. 7E) but greater pit field area per unit cell interface area (Fig. 7I) and PD per unit cell interface area (Fig. 7K) in low light plants. Meanwhile, lower PD connections between M and BS in leaves of two-week old low light-grown *Z. mays* was a result of having fewer PD per unit pit field area (Figs. 5M-P, 7G) and fewer pit fields (Figs. 5Q-T, 7I).

Plasmodesmata connections between mesophyll

Except for *S. viridis* M-M pit field area, there was significant growth irradiance, plant age, and interaction effect in all M-M PD parameters in both *S. viridis* and *Z. mays* (Table 1). In *S. viridis*, greater pit field area per unit cell interface area (Fig. 6J; Table 1) resulted to two-fold greater PD per unit cell interface area in high light plants compared to low light plants (Fig. 6L; Table 1). Meanwhile, in two week-old *Z. mays*, two-fold greater PD per unit cell interface area (Fig. 7L; Table 1) resulted from having bigger PD (Fig. 7F), more PD per unit pit field area (Fig. 7H), and greater pit field area per unit cell interface area (Fig. 7J) in high light plants compared to low light plants. In older *Z. mays*, greater pit field area per unit cell interface area (Fig. 7J) resulted to greater PD per unit cell interface area in low light plants compared to high light plants (Fig. 7L; Table 1).

Discussion

The effect of growth irradiance on C_4 leaf PD density depends on plant age and species

Despite the suggestion that C_4 plants are less plastic than C_3 plants due to their complex biochemical and anatomical attributes (Sage and McKown, 2006), there have been numerous reports on C_4 species being capable of acclimation response and plasticity to growth irradiance (Kromdijk et al., 2008; Pengelly et al., 2010; Sonawane et al., 2018; Tazoe et al., 2008). Similarly, our results showed that when NADP-ME species, *S. viridis* and *Z. mays*, were grown under different irradiances, there was a species-specific difference and an overall significant plant age effect in leaf PD density.

For a given plant developmental stage where the difference in M-BS PD area per unit leaf area between low light-grown and high light-grown plants is at least two-fold (as in seven-week old *S. viridis* and in two-week old *Z. mays*), there is also an observed significant difference in BS chloroplasts content. This finding supports a previous report (Wang et al., 2017) which suggested that chloroplast development and function are strongly coordinated with PD function and formation in bundle sheath cells (Brunkard et al., 2013). We also found that the overall lower M-BS PD area per unit leaf area in low light-grown plants was largely attributed to impaired pit

field formation manifested by lower pit field coverage, smaller pit fields, and smaller PD. It is believed that the primary PD formed during cytokinesis are pit field initials (Giannoutsou et al., 2013) and that pit fields are formed as a result of primary PD modification and/or secondary PD formation that happens later in development (Ehlers and Kollmann, 2001; Faulkner et al., 2008). Addition of PD during primary PD modification and/or secondary PD formation would entail resource and energy costs which plants with more source leaves grown under non-limiting light could energetically accommodate (Supplementary Fig. 2). On that same note, having thin cell walls might also be an advantage for PD development. However, in this study this is not supported as low light-grown plants which had thinner M and BS cell walls also had fewer PD.

While it is not possible to make firm conclusions from only two species, it is tempting to speculate that these two C_4 species may have evolved different acclimation responses to low light associated with their C_4 lineage. *S. viridis* is a member of the subtribe Cenchrinae of the MPC C_4 lineage while *Z. mays* is from the subtribe and C_4 lineage, Andropogoneae (GPWGII, 2012). This hypothesis agrees with the subtype-dependent and species-specific responses observed in other growth irradiance studies performed in C_4 plants. For instance, a previous comparison between *Z. mays* and another NADP-ME C_4 grass, *Paspalum conjugatum* showed two different responses to growth irradiance in terms of chlorophyll and Rubisco content, mainly attributed to their different habitats (Ward and Woolhouse, 1986) but this could also be due to C_4 lineage differences (GPWGII, 2012). Similarly, C_4 dicots belonging to different subtypes, *Amaranthus cruentus* (NAD-ME) (Tazoe et al., 2006) and *Flaveria bidentis* (NADP-ME) (Pengelly et al., 2010), showed contrasting responses to growth irradiance in terms of chlorophyll content. It would be very interesting to see if members of the same subtribe and/or C_4 lineage have similar patterns of leaf phenotypic response to growth irradiance.

There is not a tight link between PD density and photosynthetic capacity

In this study, plant age had no effect on photosynthetic rates of the youngest fully expanded leaves but there was an obvious difference in PD density between these developmental stages. This observation, and the lack of correspondence between

PD density and photosynthetic flux under different growth irradiances, is summarised in Figure 8. Here, the response of photosynthetic flux to incident light intensity is calculated per M-BS interface PD at the two developmental stages and at the two growth irradiances. If PD frequency was “adjusting” to photosynthetic flux, or indeed limiting it, one might expect these light response curves to all be similar on a flux per PD basis regardless of age or treatment. This is clearly not the case. One must assume that these leaves are capable of maintaining M-BS fluxes of C_4 acids and C_3 products by tolerating considerable variation in diffusion gradients across this interface and hence tolerate widely different levels of metabolites in the two compartments (Hatch and Osmond, 1976). While it is difficult to directly measure metabolite gradients in C_4 leaves, whole leaf metabolite measurements and recent work using non-aqueous fractionation and stable isotope labelling (Arrivault et al., 2017; Leegood and von Caemmerer, 1988) support this hypothesis. This is also true when comparing C_4 species where PD densities between M and BS cells vary between 5 and 12 PD μm^{-2} cell interface (Danila et al., 2018) despite these species all having similar photosynthetic rates (Pinto et al., 2014).

Light affects starch formation but not grana development in C_4 BS chloroplasts

In C_3 species, increased grana development is often observed in plants grown under low light to maximise light capture under limiting environment (Björkman, 1981). However, in this study, there was no overall enhancement in grana formation observed in M or BS chloroplasts of low light plants. This could be because of the complexity of the energy requirements of metabolism across the two cell types. It has been proposed that plasticity in decarboxylation mechanism, the form of the C_4 acid transported to the BS and the shuttling of 3-PGA from the BS to the M chloroplasts for reduction might all be ways in which energy balance could be maintained under low irradiance in C_4 leaves (Furbank, 2011; Sharwood et al., 2014; von Caemmerer and Furbank, 2016). Previous studies had also shown that when NADP-ME type C_4 plants were grown under low light, the activity and protein expression of both the decarboxylating enzyme NADP-ME (Sharwood et al., 2014; Sonawane et al., 2018) and rubisco (Sharwood et al., 2014) were proportionally reduced.

Meanwhile, accumulation of more and larger starch grains in the chloroplasts of low light *S. viridis* and *Z. mays* leaves were somewhat surprising as growth at low irradiance in most plants results in a reduction in starch levels (Zeeman et al., 2004). Our study, however, was not the first to show this as similar observations were also reported in low light-grown *Z. mays* and *Digitaria sanguinalis* from an independent study (Sowiński et al., 2007). Interestingly, these results were only observed in NADP-ME species but not in species belonging to NAD-ME or PCK subtypes (Sowiński et al., 2007). It is possible that the specialised metabolism of the NADP-ME type C_4 grasses plays a role in the availability of energy to fuel carbohydrate export from the bundle sheath or perhaps there are other unique biochemical features in the starch synthesis and degradation pathways in plants of this decarboxylation type (Ma et al., 2009; Russin et al., 1996; Slewinski et al., 2009).

Concluding Comments

The observation that PD density at the M-BS cell interface is greatly enhanced in C_4 leaves compared to C_3 leaves (Danila et al., 2016; Danila et al., 2018) to support C_4 photosynthetic metabolite flux would imply some functional relationship between PD density and photosynthetic capacity. While the data presented here indicate that there was some plasticity in PD density of C_4 leaves in response to growth irradiance, there was no clear correlation found between either photosynthetic capacity or photosynthetic flux and PD density at the M-BS cell interface. These results suggest a complex mechanism underlying the dynamic response of C_4 leaf PD formation to growth irradiance.

References

Arrivault, S., Obata, T., Szecówka, M., Mengin, V., Guenther, M., Hoehne, M., Fernie, A.R., Stitt, M., 2017. Metabolite pools and carbon flow during C4 photosynthesis in maize: 13CO2 labeling kinetics and cell type fractionation. Journal of Experimental Botany 68, 283-298.

Björkman, O., 1981. Responses to Different Quantum Flux Densities, in: Lange, O.L., Nobel, P.S., Osmond, C.B., Ziegler, H. (Eds.), Physiological Plant Ecology I: Responses to the Physical Environment. Springer Berlin Heidelberg, Berlin, Heidelberg, pp. 57-107.

Botha, C.E.J., 1992. Plasmodesmatal distribution, structure and frequency in relation to assimilation in C_3 and C_4 grasses in southern Africa. Planta 187, 348-358.

Brunkard, J.O., Runkel, A.M., Zambryski, P.C., 2013. Plasmodesmata dynamics are coordinated by intracellular signaling pathways. Current opinion in plant biology 16, 10.1016/j.pbi.2013.1007.1007.

Brutnell, T.P., Wang, L., Swartwood, K., Goldschmidt, A., Jackson, D., Zhu, X.-G., Kellogg, E., Van Eck, J., 2010. Setaria viridis: A Model for C(4) Photosynthesis. The Plant Cell 22, 2537-2544.

Danila, F.R., Quick, W.P., White, R.G., Furbank, R.T., von Caemmerer, S., 2016. The Metabolite Pathway between Bundle Sheath and Mesophyll: Quantification of Plasmodesmata in Leaves of C(3) and C(4) Monocots. The Plant Cell 28, 1461-1471.

Danila, F.R., Quick, W.P., White, R.G., Kelly, S., von Caemmerer, S., Furbank, R.T., 2018. Multiple mechanisms for enhanced plasmodesmata density in disparate subtypes of C4 grasses. Journal of Experimental Botany 69, 1135-1145.

Ehlers, K., Kollmann, R., 2001. Primary and secondary plasmodesmata: structure, origin, and functioning. Protoplasma 216, 1-30.

Faulkner, C., Akman, O.E., Bell, K., Jeffree, C., Oparka, K., 2008. Peeking into Pit Fields: A Multiple Twinning Model of Secondary Plasmodesmata Formation in Tobacco. The Plant Cell 20, 1504-1518.

Furbank, R., Jenkins, C., Hatch, M., 1990. C₄ Photosynthesis: Quantum Requirement, C₄ acid overcycling and <I>Q</I>-Cycle Involvement. Functional Plant Biology 17, 1-7.

Furbank, R.T., 2011. Evolution of the C4 photosynthetic mechanism: are there really three C4 acid decarboxylation types? Journal of Experimental Botany 62, 3103-3108.

Giannoutsou, E., Sotiriou, P., Apostolakos, P., Galatis, B., 2013. Early local differentiation of the cell wall matrix defines the contact sites in lobed mesophyll cells of Zea mays. Annals of Botany 112, 1067-1081.

GPWGII, 2012. New grass phylogeny resolves deep evolutionary relationships and discovers C_4 origins. New Phytologist 193, 304-312.

Gunning, B.E.S., 1978. Age-related and origin-related control of the numbers of plasmodesmata in cell walls of developing Azolla roots. Planta 143, 181-190.

Hatch, M.D., 1987. C_4 photosynthesis: a unique blend of modified biochemistry, anatomy and ultrastructure. Biochimica et Biophysica Acta (BBA) - Reviews on Bioenergetics 895, 81-106.

Hatch, M.D., Osmond, C.B., 1976. Compartmentation and Transport in C4 Photosynthesis, in: Stocking, C.R., Heber, U. (Eds.), Transport in Plants III. Springer Berlin Heidelberg, pp. 144-184.

Henderson, S., Caemmerer, S., Farquhar, G., 1992. Short-Term Measurements of Carbon Isotope Discrimination in Several C₄ Species. Functional Plant Biology 19, 263-285.

Kromdijk, J., Schepers, H.E., Albanito, F., Fitton, N., Carroll, F., Jones, M.B., Finnan, J., Lanigan, G.J., Griffiths, H., 2008. Bundle Sheath Leakiness and Light Limitation during C₄ Leaf and Canopy CO₂ Uptake. Plant Physiology 148, 2144-2155.

Leegood, R.C., von Caemmerer, S., 1988. The relationship between contents of photosynthetic metabolites and the rate of photosynthetic carbon assimilation in leaves of Amaranthus edulis L. Planta 174, 253-262.

Li, P., Brutnell, T.P., 2011. Setaria viridis and Setaria italica, model genetic systems for the Panicoid grasses. Journal of Experimental Botany 62, 3031-3037.

Lu, K.J., Danila, F.R., Cho, Y., Faulkner, C., 2018. Peeking at a plant through the holes in the wall – exploring the roles of plasmodesmata. New Phytologist 0.

Ma, Y., Slewinski, T.L., Baker, R.F., Braun, D.M., 2009. Tie-dyed1 Encodes a Novel, Phloem-Expressed Transmembrane Protein That Functions in Carbohydrate Partitioning. Plant Physiology 149, 181-194.

Pengelly, J.J.L., Sirault, X.R.R., Tazoe, Y., Evans, J.R., Furbank, R.T., von Caemmerer, S., 2010. Growth of the C_4 dicot Flaveria bidentis: photosynthetic acclimation to low light through shifts in leaf anatomy and biochemistry. Journal of Experimental Botany 61, 4109-4122.

Pinto, H., Sharwood, R.E., Tissue, D.T., Ghannoum, O., 2014. Photosynthesis of C(3), C(3)–C(4), and C(4) grasses at glacial CO(2). Journal of Experimental Botany 65, 3669-3681.

Porra, R.J., Thompson, W.A., Kriedemann, P.E., 1989. Determination of accurate extinction coefficients and simultaneous equations for assaying chlorophylls a and b extracted with four different solvents: verification of the concentration of chlorophyll standards by atomic absorption spectroscopy. Biochimica et Biophysica Acta (BBA) - Bioenergetics 975, 384-394.

518 Russin, W.A., Evert, R.F., Vanderveer, P.J., Sharkey, T.D., Briggs, S.P., 1996.
519 Modification of a Specific Class of Plasmodesmata and Loss of Sucrose Export
520 Ability in the sucrose export defective1 Maize Mutant. The Plant Cell 8, 645-658.

521 Sage, R.F., McKown, A.D., 2006. Is C4 photosynthesis less phenotypically plastic
522 than C3 photosynthesis?*. Journal of Experimental Botany 57, 303-317.

523 Sage, R.F., Pearcy, R.W., 2000. The Physiological Ecology of C4 Photosynthesis, in:
524 Leegood, R.C., Sharkey, T.D., von Caemmerer, S. (Eds.), Photosynthesis:
525 Physiology and Metabolism. Springer Netherlands, Dordrecht, pp. 497-532.

526 Seagull, R.W., 1983. Differences in the frequency and disposition of plasmodesmata
527 resulting from root cell elongation. Planta 159, 497-504.

528 Sharwood, R.E., Sonawane, B.V., Ghannoum, O., 2014. Photosynthetic flexibility in
529 maize exposed to salinity and shade. Journal of Experimental Botany 65, 3715-3724.

530 Slewinski, T.L., Meeley, R., Braun, D.M., 2009. Sucrose transporter1 functions in
531 phloem loading in maize leaves. Journal of Experimental Botany 60, 881-892.

532 Sonawane, B.V., Sharwood, R.E., Whitney, S., Ghannoum, O., 2018. Shade
533 compromises the photosynthetic efficiency of NADP-ME less than that of PEP-CK
534 and NAD-ME C4 grasses. Journal of Experimental Botany 69, 3053-3068.

535 Sowiński, P., Bilska, A., Barańska, K., Fronk, J., Kobus, P., 2007. Plasmodesmata
536 density in vascular bundles in leaves of C_4 grasses grown at different light conditions
537 in respect to photosynthesis and photosynthate export efficiency. Environmental and
538 Experimental Botany 61, 74-84.

539 Tangl, E., 1879. ober offene Kommunikation zwischen den Zellen des Endosperms
540 einiger Samen. Jb Wiss Bot 12, 170-190.

541 Tazoe, Y., Hanba, Y.T., Furumoto, T., Noguchi, K., Terashima, I., 2008.
542 Relationships Between Quantum Yield for CO2 Assimilation, Activity of Key
543 Enzymes and CO2 Leakiness in Amaranthus cruentus, a C4 Dicot, Grown in High or
544 Low Light. Plant and Cell Physiology 49, 19-29.

545 Tazoe, Y., Noguchi, K., Terashima, I., 2006. Effects of growth light and nitrogen
546 nutrition on the organization of the photosynthetic apparatus in leaves of a C4 plant,
547 Amaranthus cruentus. Plant, Cell & Environment 29, 691-700.

548 von Caemmerer, S., Furbank, R., 2003. The C_4 pathway: an efficient CO_2 pump.
549 Photosynthesis Research 77, 191-207.

550 von Caemmerer, S., Furbank, R.T., 2016. Strategies for improving C4
551 photosynthesis. Current Opinion in Plant Biology 31, 125-134.

552 Wang, P., Khoshravesh, R., Karki, S., Tapia, R., Balahadia, C.P., Bandyopadhyay,
553 A., Quick, W.P., Furbank, R.T., Sage, T.L., Langdale, J.A., 2017. Re-creation of a
554 key step in the evolutionary switch from C3 to C4 leaf anatomy. Current Biology 27,
555 3278-3287.

556 Ward, D.A., Woolhouse, H.W., 1986. Comparative effects of light during growth on
557 the photosynthetic properties of NADP-ME type C4 grasses from open and shaded

habitats. I. Gas exchange, leaf anatomy and ultrastructure*. Plant, Cell & Environment 9, 261-270.

Zeeman, S.C., Smith, S.M., Smith, A.M., 2004. The breakdown of starch in leaves. New Phytologist 163, 247-261.

Figure legends

Figure 1. Light response curves of gross CO_2 assimilation of *Setaria viridis* (A) and *Zea mays* (B) grown under different irradiances. High light (HL) at 1000 µmol m^{-2} s^{-1} and low light (LL) at 100 µmol m^{-2} s^{-1}. Photosynthetic measurement was done on the middle portion of the youngest fully expanded leaf of plants at two weeks (2w) and seven weeks after germination (7w) plants. Gross CO_2 assimilation rates of *S. viridis* and *Z. mays* measured at growth irradiances are plotted in (C) and (D), respectively. Each symbol or bar represents the mean ± SE, n=3. Letters indicate the ranking (lowest=a) using multiple-comparison Tukey's post-hoc test. Bars with same letter are not statistically different at $P<0.05$. Mean dark respiration rates and corresponding statistical analysis were provided in Supplementary Figure 3 and Table 1, respectively.

Figure 2. Leaf properties of *S. viridis* grown under different irradiances. Low light at 100 µmol m^{-2} s^{-1} and high light at 1000 µmol m^{-2} s^{-1}. Embedded values on (C) correspond to chlorophyll a/b ratio. All measurements were done using the middle portion of the youngest fully expanded leaf harvested immediately after gas exchange measurement. Letters indicate the ranking (lowest=a) using multiple-comparison Tukey's post-hoc test. Bars with same letter are not statistically different at $P<0.05$. N, nitrogen; BS, bundle sheath; M, mesophyll.

Figure 3. Leaf properties of *Z. mays* grown under different irradiances. Details and statistics are as described in Fig. 2.

Figure 4. Leaf micrographs of *S. viridis* grown under different irradiances. Low light at 100 µmol m^{-2} s^{-1} and high light at 1000 µmol m^{-2} s^{-1}. Light micrographs (A-D) were generated using the middle portion of the youngest fully expanded leaf harvested immediately after gas exchange measurement. Corresponding transmission electron micrographs (TEM) of bundle sheath (BS) chloroplasts (E-H) and mesophyll (M) chloroplasts (I-L) were obtained. Pit field size (white outline in scanning electron micrographs (SEM)) (M-P) and pit field (green fluorescence in confocal micrographs) distribution (Q-T) between M and BS were also shown. s, starch grain. Light

625 micrograph bars = 25 μm. TEM bars = 1 μm, confocal micrograph bars = 10 μm,
626 SEM bars = 0.5 μm.
627
628 **Figure 5.** Leaf micrographs of *Z. mays* grown under different irradiances. Details are
629 as described in Fig. 4.
630
631 **Figure 6.** Leaf plasmodesmata (PD) properties of *S. viridis* grown under different
632 irradiances. Low light at 100 μmol m^{-2} s^{-1} and high light at 1000 μmol m^{-2} s^{-1}. All
633 measurements were done using the middle portion of the youngest fully expanded
634 leaf harvested immediately after gas exchange measurement. Letters indicate the
635 ranking (lowest=a) using multiple-comparison Tukey's post-hoc test. Bars with same
636 letter are not statistically different at $P<0.05$. M, mesophyll; BS, bundle sheath; S_b,
637 bundle sheath surface area per leaf unit area.
638
639 **Figure 7.** Leaf plasmodesmata (PD) properties of *Z. mays* grown under different
640 irradiances. Details and statistics are as described in Fig. 6.
641
642 **Figure 8.** Light response curves of plasmodesmata (PD) flux between mesophyll
643 and bundle sheath cells of *S. viridis* (A) and *Z. mays* (B) grown under different
644 irradiances. Calculations as previously described in (Danila et al., 2016). Gross CO_2
645 assimilation rate per PD assumes that in C_4 species the minimum flux of C_4 acids
646 through the PD needs to be equal to or greater than the gross CO_2 assimilation rate
647 (Henderson et al., 1992). See Figure 1 for details.
648
649 **Supplementary Figure 1.** Relationship between gross CO_2 assimilation rate and
650 total leaf N content of *S. viridis* and *Z. mays* grown under different irradiances. Low
651 light (LL) at 100 μmol m^{-2} s^{-1} and high light (HL) at 1000 μmol m^{-2} s^{-1}.
652
653 **Supplementary Figure 2.** Seven week-old *S. viridis* and *Z. mays* grown under
654 different irradiances. Low light at 100 μmol m^{-2} s^{-1} and high light at 1000 μmol m^{-2} s^{-1}.
655 (A) Low light-grown *S. viridis*, (B) high light-grown *S. viridis,* (C) low light-grown *Z.*
656 *mays*, and (D) high light-grown *Z. mays*. Red arrowhead points to the leaf used for
657 measurements and quantification. Bar = 20 cm.

Supplementary Figure 3. Dark respiration rates of *S. viridis* (A) and *Z. mays* (B) grown under different growth irradiances. Each bar represents the mean ± SE, n=3. Letters indicate the ranking (lowest=a) using multiple-comparison Tukey's post-hoc test. Bars with same letter are not statistically different at $P<0.05$.

Tables

Table 1. Summary of statistical analysis using two-way ANOVA to test for the effects of growth irradiance and plant age to various response parameters.

Parameter	*S. viridis*			*Z. mays*		
	Irradiance	Age	Irradiance x Age	Irradiance	Age	Irradiance x Age
A_{gross} (µmol CO_2 m^{-2} s^{-1})	***	ns	ns	***	**	*
R_d (µmol CO_2 m^{-2} s^{-1})	**	*	ns	***	**	ns
LMA (g m^{-2})	***	**	ns	***	***	***
Total leaf N (mmol m^{-2})	***	ns	ns	***	***	**
Chl a+b (µmol m^{-2})	**	**	ns	*	*	ns
Chl a/b	***	*	ns	***	ns	***
BS chloroplast content (%)	ns	***	*	*	ns	ns
BS chloroplast size (µm^2)	ns	ns	***	***	**	***
M chloroplast size (µm^2)	ns	***	ns	***	ns	ns
BS grana width (µm)	ns	ns	**	ns	*	ns
M grana width (µm)	**	***	***	*	***	ns
BS starch granule per chloroplast	***	***	***	***	ns	ns
M starch granule per chloroplast	***	***	***	*	*	*
BS starch granule size (µm^2)	***	***	***	***	ns	***
M starch granule size (µm^2)	***	***	***	***	***	***
Vein circumference (µm)	***	ns	***	***	ns	***
Interveinal distance (µm)	***	ns	***	***	***	*
Leaf thickness (µm)	***	*	***	***	ns	***
BS cell wall thickness (µm)	***	ns	ns	***	***	***
M cell wall thickness (µm)	***	**	ns	***	**	ns
S_b (m^2 m^{-2})	***	***	**	ns	**	ns
M-BS PD area per unit leaf area (m^2 m^{-2})	***	***	***	***	***	***
M-BS pit field area (µm^2)	**	ns	**	**	**	ns
M-M pit field area (µm^2)	ns	ns	ns	*	ns	***
M-BS PD area (µm^2)	ns	***	***	**	***	***
M-M PD area (µm^2)	ns	***	*	***	*	***
M-BS PD per unit pit field area (PD µm^{-2})	***	***	***	***	ns	***
M-M PD per unit pit field area (PD µm^{-2})	***	***	***	***	***	***
M-BS pit field area per cell interface area (%)	***	***	***	***	**	***
M-M pit field area per cell interface area (%)	***	***	***	ns	***	***
M-BS PD per unit cell interface area (PD µm^{-2})	***	***	***	***	ns	***
M-M PD per unit cell interface area (PD µm^{-2})	***	***	***	***	***	***

ns, not significant (P>0.05); *P<0.05; **P<0.01; ***P<0.001. A_{gross}, gross CO_2 assimilation rate; R_d, dark respiration rate; LMA, leaf mass per area; Chl, chlorophyll; BS, bundle sheath; M, mesophyll; S_b, bundle sheath surface area per unit leaf area; PD, plasmodesmata.

Table 2. Chloroplast properties of *S. viridis* grown under low (100 µmol m^{-2} s^{-1}) and high (1000 µmol m^{-2} s^{-1}) irradiances.

Parameter	*S. viridis*			
	2-week old		7-week old	
	Low	High	Low	High
BS chloroplast size (µm²), n=39	19.6 ± 1.07^{ab}	25.6 ± 1.76^{c}	22.8 ± 1.52^{bc}	16.5 ± 1.73^{a}
M chloroplast size (µm²), n=12	21.2 ± 1.93^{ab}	25.2 ± 2.46^{b}	16.6 ± 1.71^{a}	15.9 ± 1.33^{a}
BS grana width (µm), n=47	0.09 ± 0.007^{a}	0.12 ± 0.004^{b}	0.11 ± 0.009^{ab}	0.10 ± 0.004^{b}
M grana width (µm), n=120	0.32 ± 0.012^{a}	0.33 ± 0.014^{a}	0.45 ± 0.024^{b}	0.35 ± 0.015^{a}
BS starch granule per chloroplast, n=39	15 ± 1.1^{b}	6 ± 0.4^{a}	5 ± 0.5^{a}	4 ± 0.4^{a}
M starch granule per chloroplast, n=12	8 ± 0.9^{b}	1 ± 0.4^{a}	2 ± 0.5^{a}	0 ± 0.0^{a}
BS starch granule size (µm²), n=125	0.27 ± 0.007^{c}	0.08 ± 0.003^{a}	0.15 ± 0.006^{b}	0.06 ± 0.003^{a}
M starch granule size (µm²), n=25	0.33 ± 0.021^{b}	0.07 ± 0.005^{a}	0.05 ± 0.007^{a}	na

The average number of corresponding structures measured is indicated by n. Letters indicate the ranking (lowest=a) of plants within each single row using multiple-comparison Tukey's post-hoc test. Values followed by the same superscript letter are not significantly different at the 5% level. BS, bundle sheath; M, mesophyll; na, not applicable.

Table 3. Chloroplast properties of *Z. mays* grown under low (100 µmol m^{-2} s^{-1}) and high (1000 µmol m^{-2} s^{-1}) irradiances.

Parameter	*Z. mays*			
	2-week old		7-week old	
	Low	High	Low	High
BS chloroplast size (µm^2), n=56	8.9 ± 0.44^a	12.5 ± 0.78^b	8.3 ± 0.39^a	17.4 ± 0.91^c
M chloroplast size (µm^2), n=30	10.8 ± 1.13^a	16.3 ± 1.13^b	11.4 ± 0.82^{ac}	15.2 ± 0.99^{bc}
BS grana width (µm), n=28	0.07 ± 0.003^a	0.07 ± 0.003^a	0.08 ± 0.006^a	0.08 ± 0.005^a
M grana width (µm), n=130	0.43 ± 0.014^a	0.49 ± 0.019^{ab}	0.54 ± 0.035^{bc}	0.58 ± 0.026^c
BS starch granule per chloroplast, n=56	4 ± 0.5^a	1 ± 0.3^b	4 ± 0.4^a	0 ± 0.0^b
M starch granule per chloroplast, n=30	0 ± 0.0^a	0 ± 0.0^a	1 ± 0.4^b	0 ± 0.0^a
BS starch granule size (µm^2), n=107	0.12 ± 0.005^a	0.07 ± 0.012^a	0.15 ± 0.005^b	na
M starch granule size (µm^2), n=34	na	na	0.09 ± 0.008^b	na

The average number of corresponding structures measured is indicated by n. Letters indicate the ranking (lowest=a) of plants within each single row using multiple-comparison Tukey's post-hoc test. Values followed by the same superscript letter are not significantly different at the 5% level. BS, bundle sheath; M, mesophyll; na, not applicable.

Figures

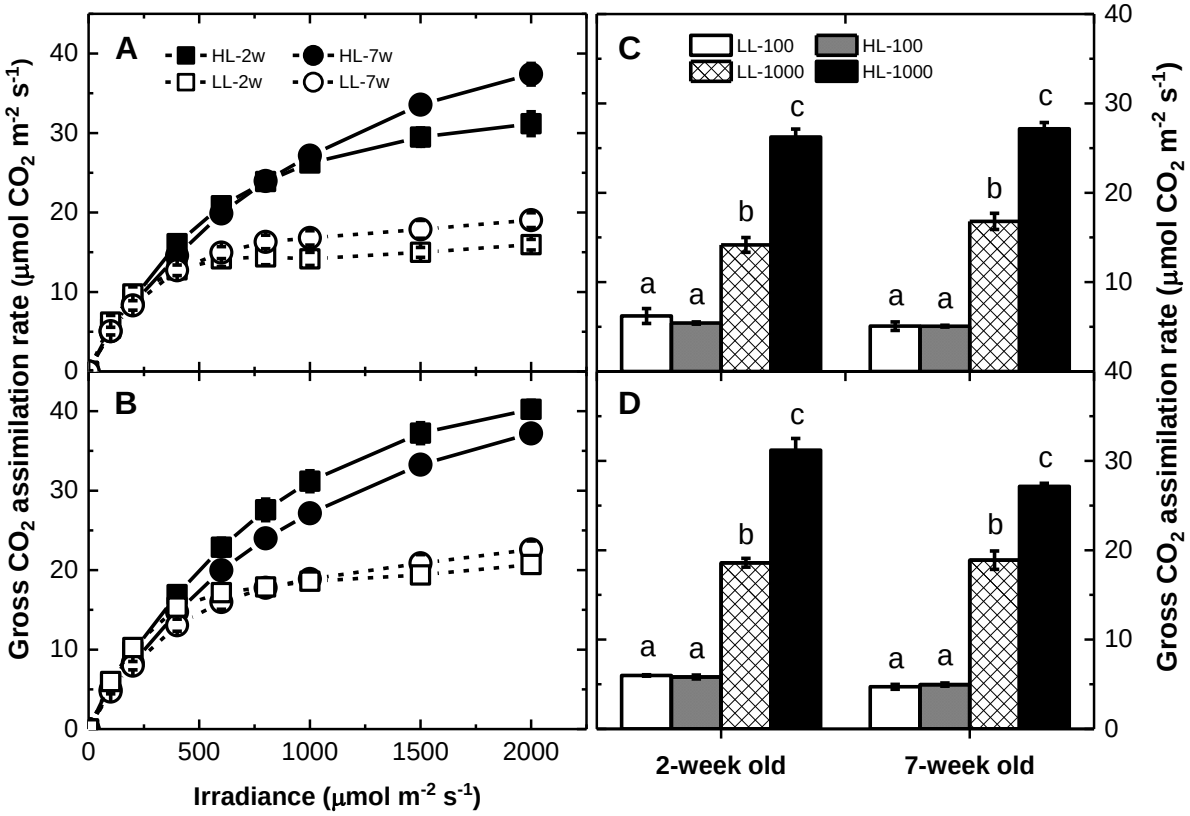

Figure 1. Light response curves of gross CO_2 assimilation of *Setaria viridis* (A) and *Zea mays* (B) grown under different irradiances. High light (HL) at 1000 μmol m^{-2} s^{-1} and low light (LL) at 100 μmol m^{-2} s^{-1}. Photosynthetic measurement was done on the middle portion of the youngest fully expanded leaf of plants at two weeks (2w) and seven weeks after germination (7w) plants. Gross CO_2 assimilation rates of *S. viridis* and *Z. mays* measured at growth irradiances are plotted in (C) and (D), respectively. Each symbol or bar represents the mean ± SE, n=3. Letters indicate the ranking (lowest=a) using multiple-comparison Tukey's post-hoc test. Bars with same letter are not statistically different at $P<0.05$. Mean dark respiration rates and corresponding statistical analysis were provided in Supplementary Figure 3 and Table 1, respectively.

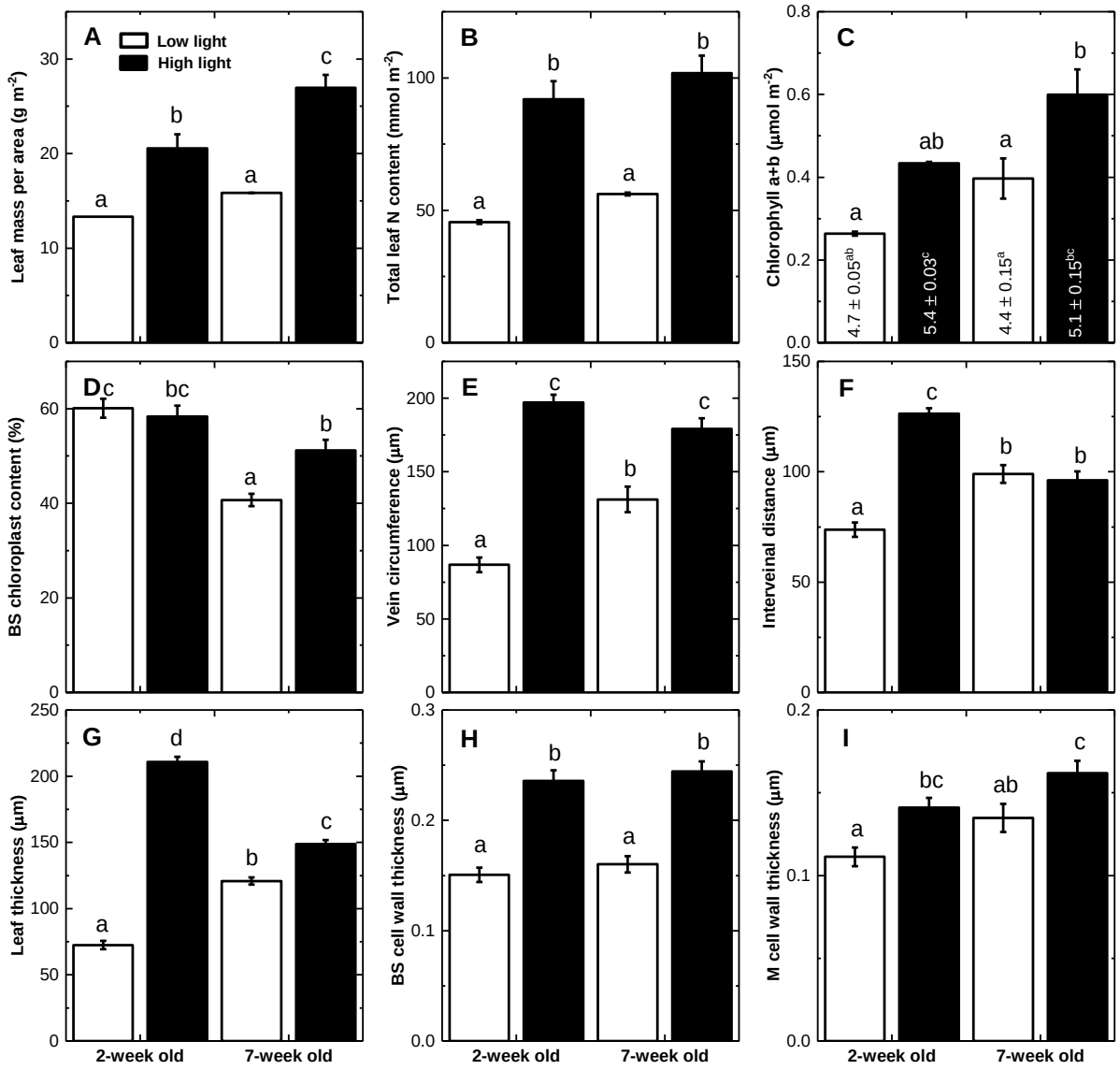

Figure 2. Leaf properties of *S. viridis* grown under different irradiances. Low light at 100 µmol m^{-2} s^{-1} and high light at 1000 µmol m^{-2} s^{-1}. Embedded values on (C) correspond to chlorophyll a/b ratio. All measurements were done using the middle portion of the youngest fully expanded leaf harvested immediately after gas exchange measurement. Letters indicate the ranking (lowest=a) using multiple-comparison Tukey's post-hoc test. Bars with same letter are not statistically different at $P<0.05$. N, nitrogen; BS, bundle sheath; M, mesophyll.

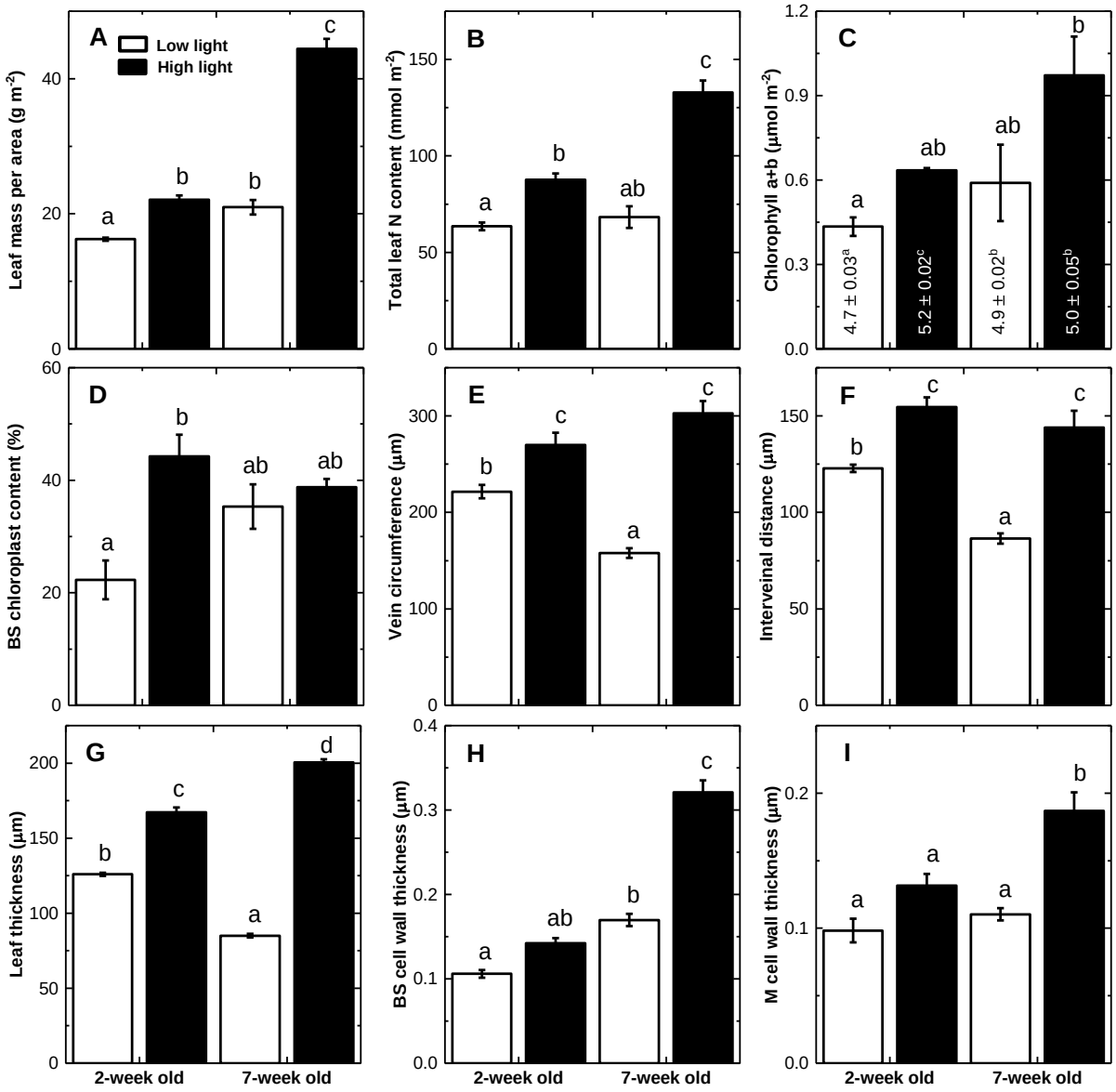

Figure 3. Leaf properties of *Z. mays* grown under different irradiances. Details and statistics are as described in Fig. 2.

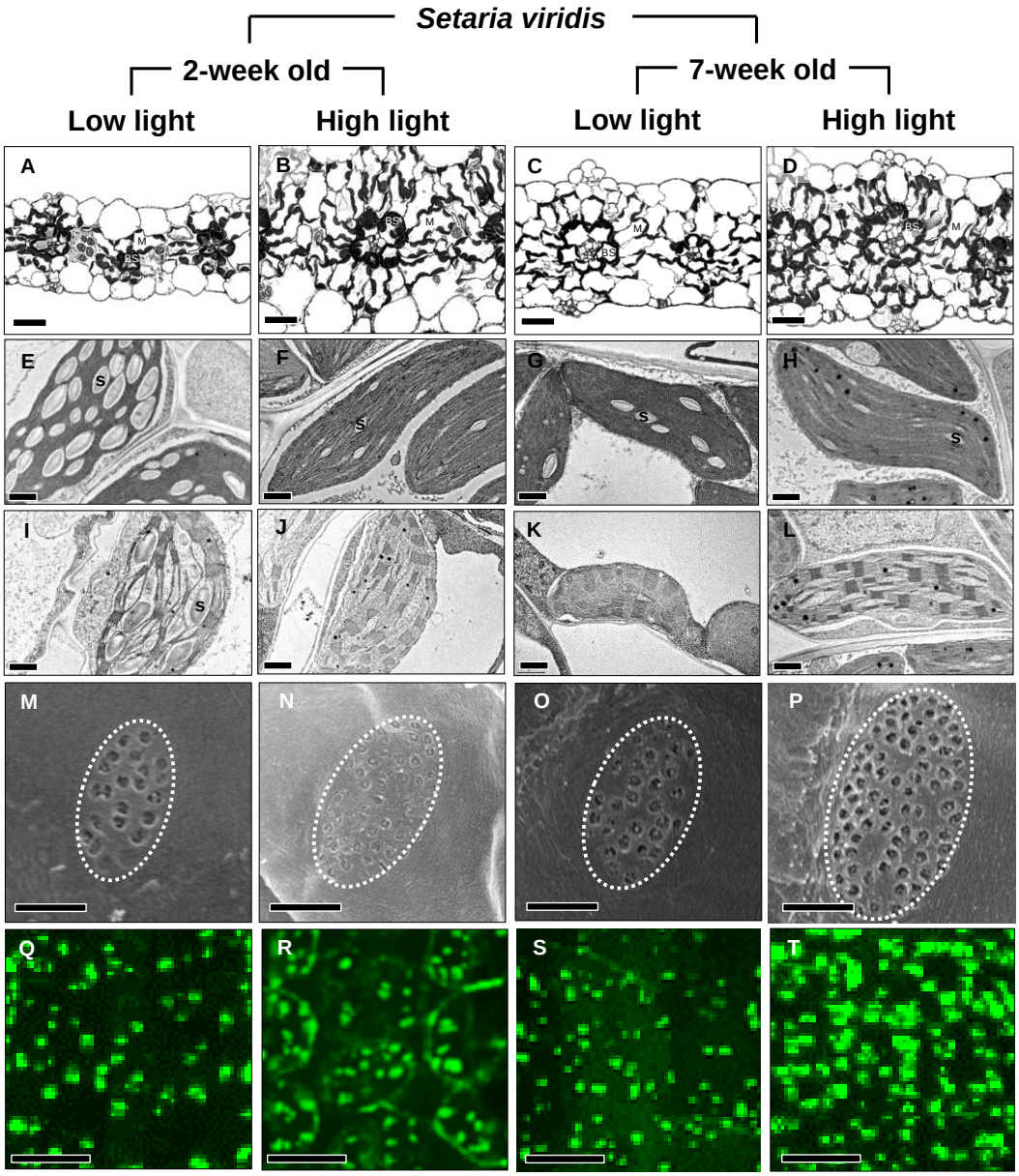

Figure 4. Leaf micrographs of *S. viridis* grown under different irradiances. Low light at 100 µmol m^{-2} s^{-1} and high light at 1000 µmol m^{-2} s^{-1}. Light micrographs (A-D) were generated using the middle portion of the youngest fully expanded leaf harvested immediately after gas exchange measurement. Corresponding transmission electron micrographs (TEM) of bundle sheath (BS) chloroplasts (E-H) and mesophyll (M) chloroplasts (I-L) were obtained. Pit field size (white outline in scanning electron micrographs (SEM)) (M-P) and pit field (green fluorescence in confocal micrographs) distribution (Q-T) between M and BS were also shown. s, starch grain. Light micrograph bars = 25 μm. TEM bars = 1 μm, confocal micrograph bars = 10 μm, SEM bars = 0.5 μm.

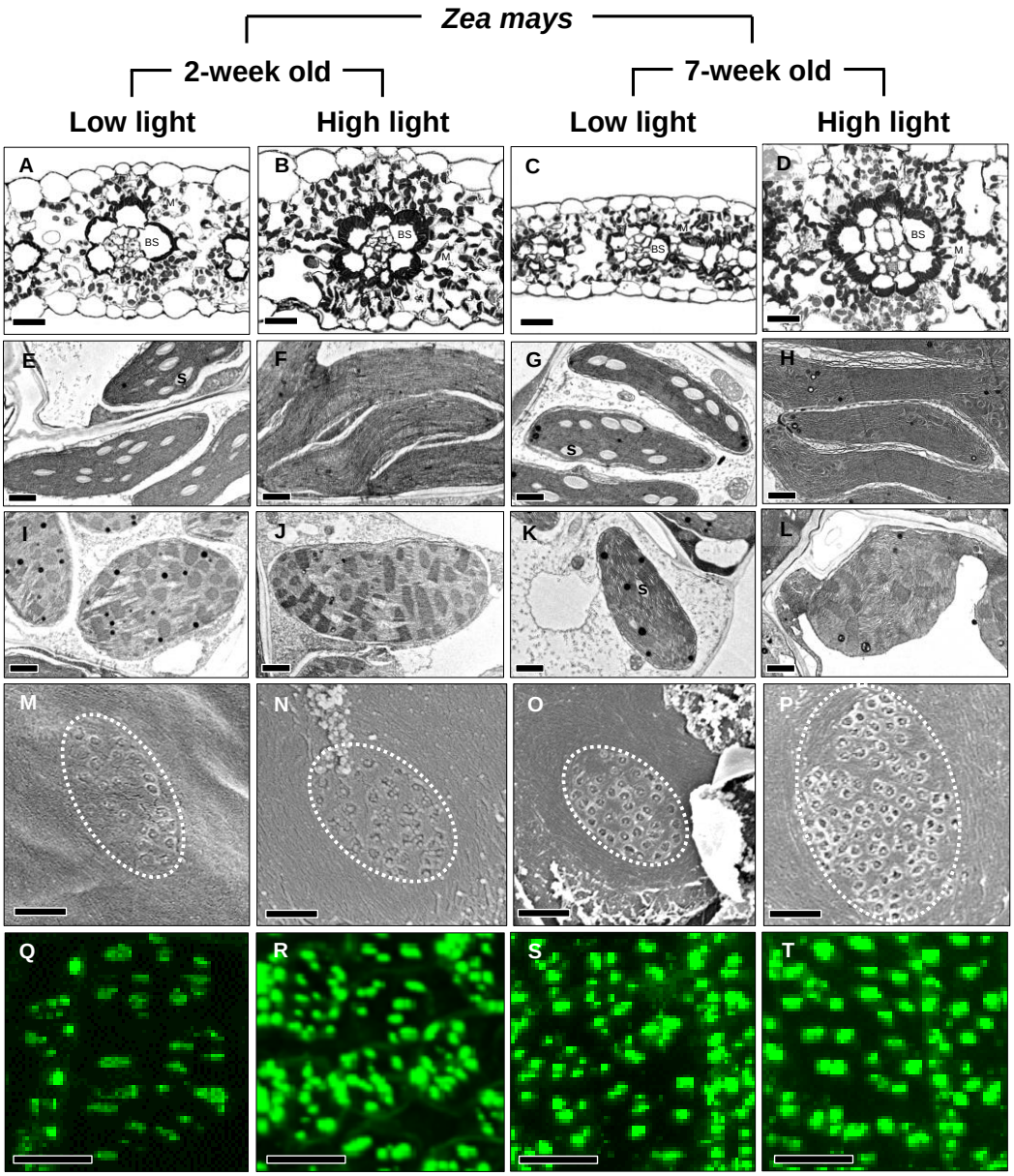

Figure 5. Leaf micrographs of *Z. mays* grown under different irradiances. Details are as described in Fig. 4.

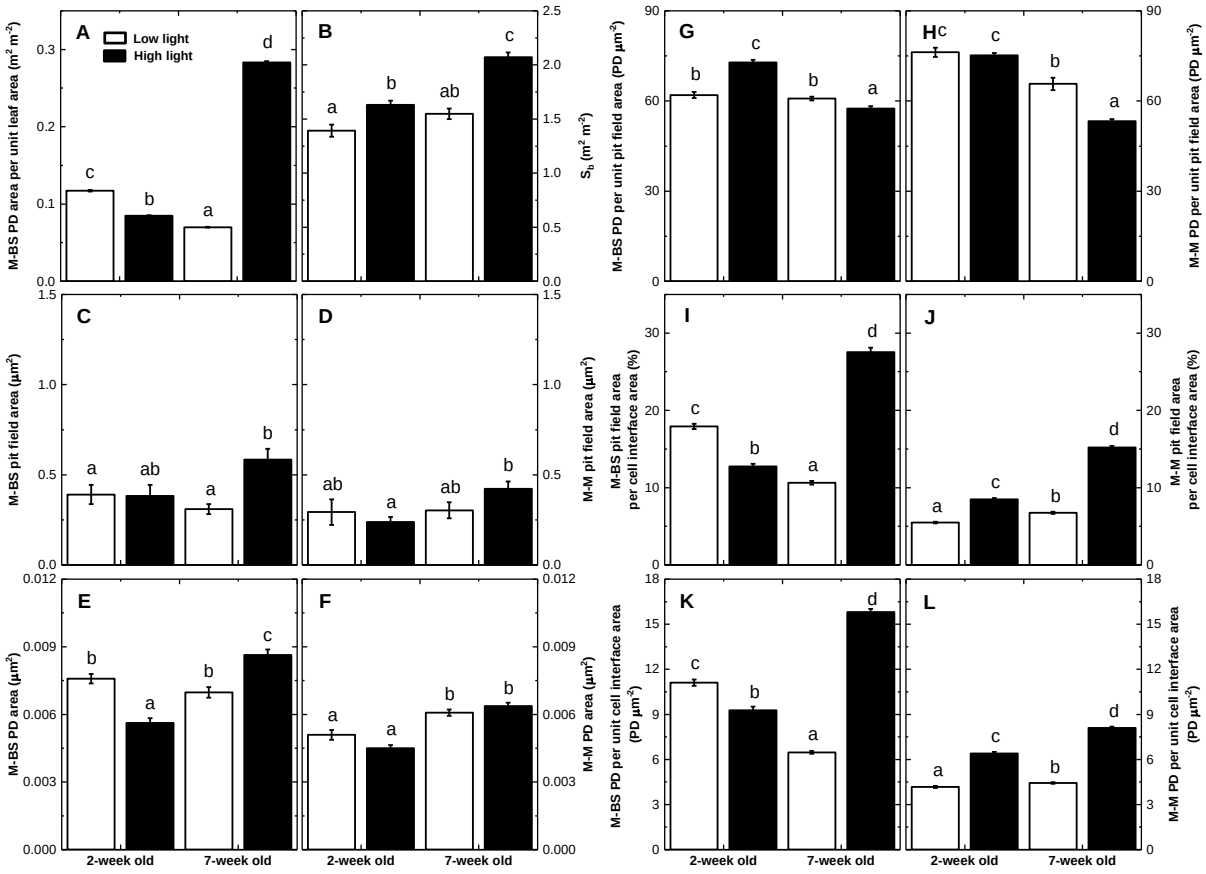

Figure 6. Leaf plasmodesmata (PD) properties of *S. viridis* grown under different irradiances. Low light at 100 µmol m^{-2} s^{-1} and high light at 1000 µmol m^{-2} s^{-1}. All measurements were done using the middle portion of the youngest fully expanded leaf harvested immediately after gas exchange measurement. Letters indicate the ranking (lowest=a) using multiple-comparison Tukey's post-hoc test. Bars with same letter are not statistically different at $P<0.05$. M, mesophyll; BS, bundle sheath; S_b, bundle sheath surface area per leaf unit area.

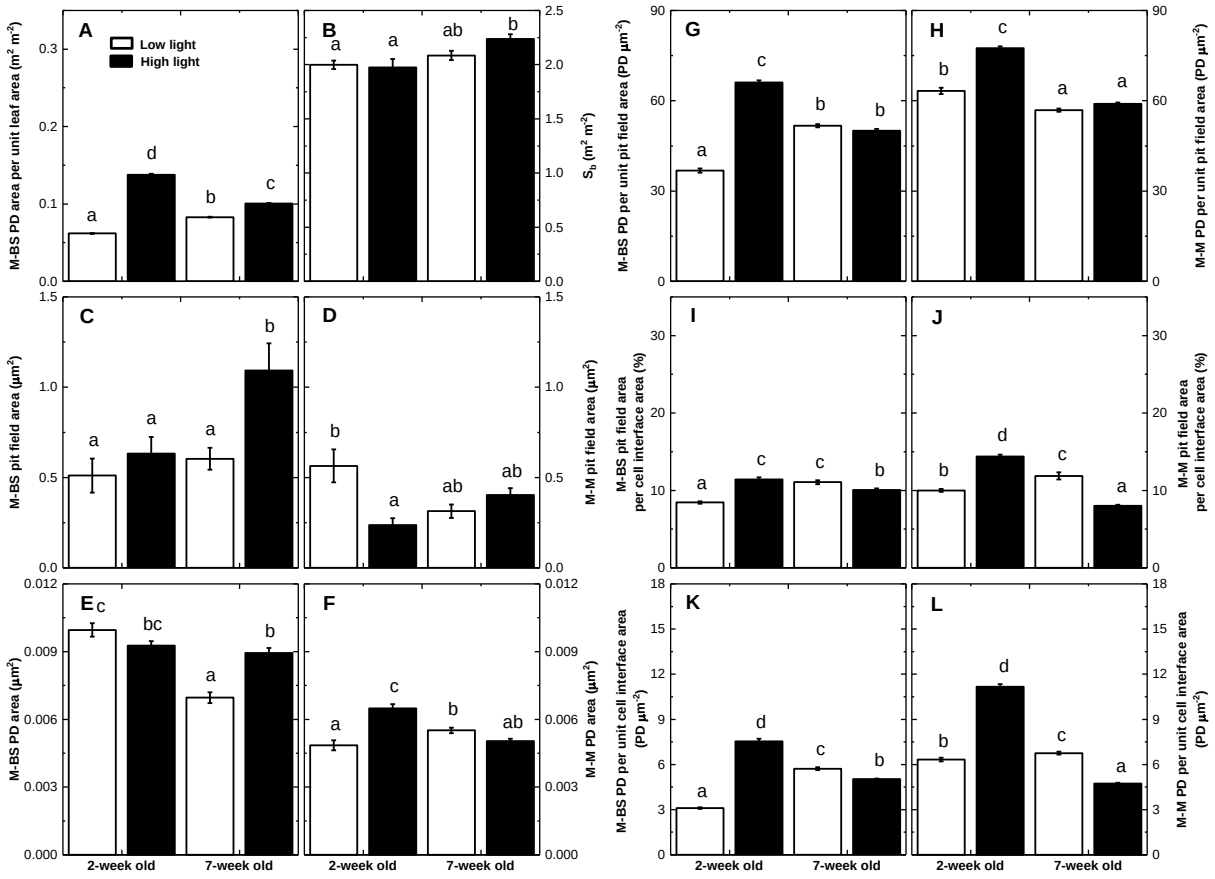

Figure 7. Leaf plasmodesmata (PD) properties of *Z. mays* grown under different irradiances. Details and statistics are as described in Fig. 6.

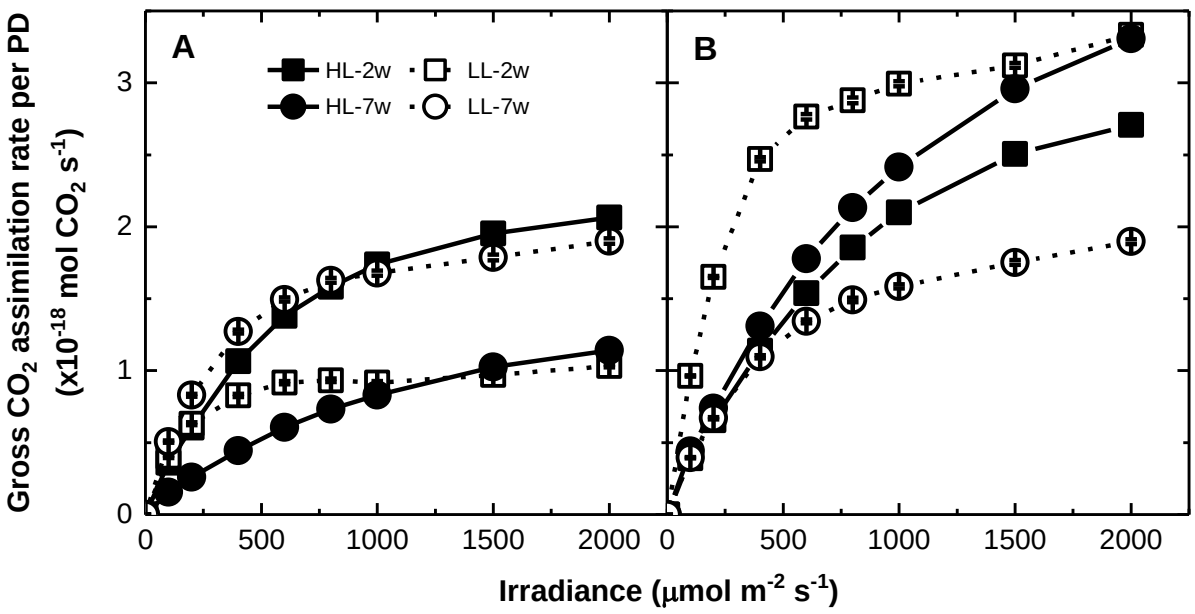

Figure 8. Light response curves of plasmodesmata (PD) flux between mesophyll and bundle sheath cells of *S. viridis* (A) and *Z. mays* (B) grown under different irradiances. Calculations as previously described in (Danila et al., 2016). Gross CO_2 assimilation rate per PD assumes that in C_4 species the minimum flux of C_4 acids through the PD needs to be equal to or greater than the gross CO_2 assimilation rate (Henderson et al., 1992). See Figure 1 for details.

Supporting information

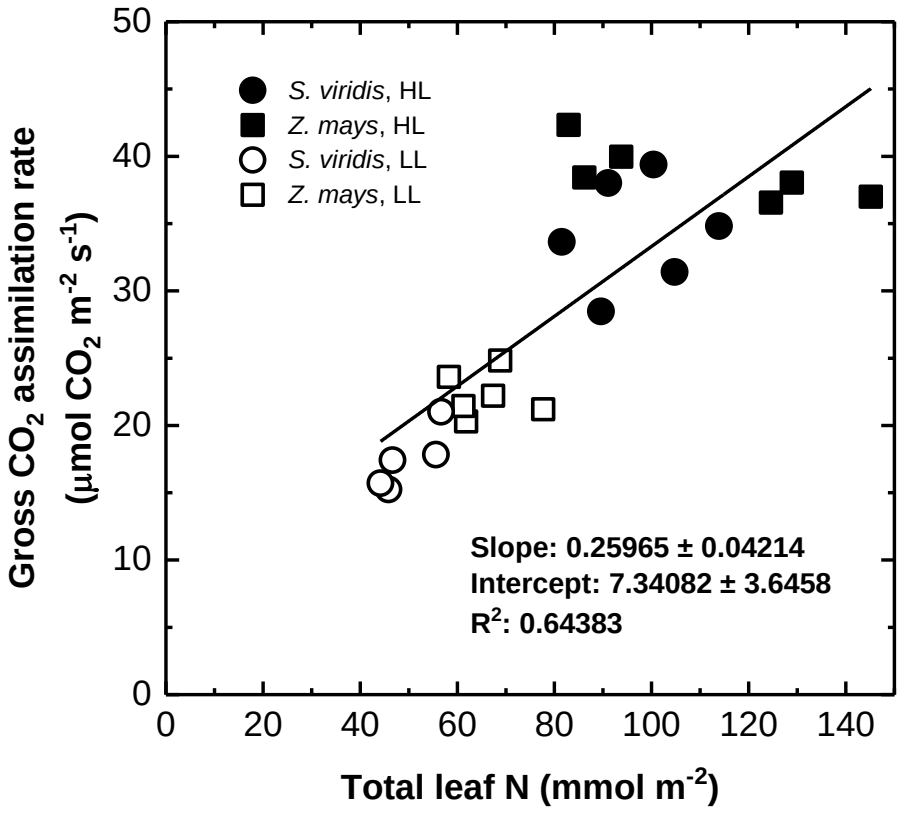

Supplementary Figure 1. Relationship between gross CO_2 assimilation rate and total leaf N content of *S. viridis* and *Z. mays* grown under different irradiances. Low light (LL) at 100 µmol m^{-2} s^{-1} and high light (HL) at 1000 µmol m^{-2} s^{-1}.

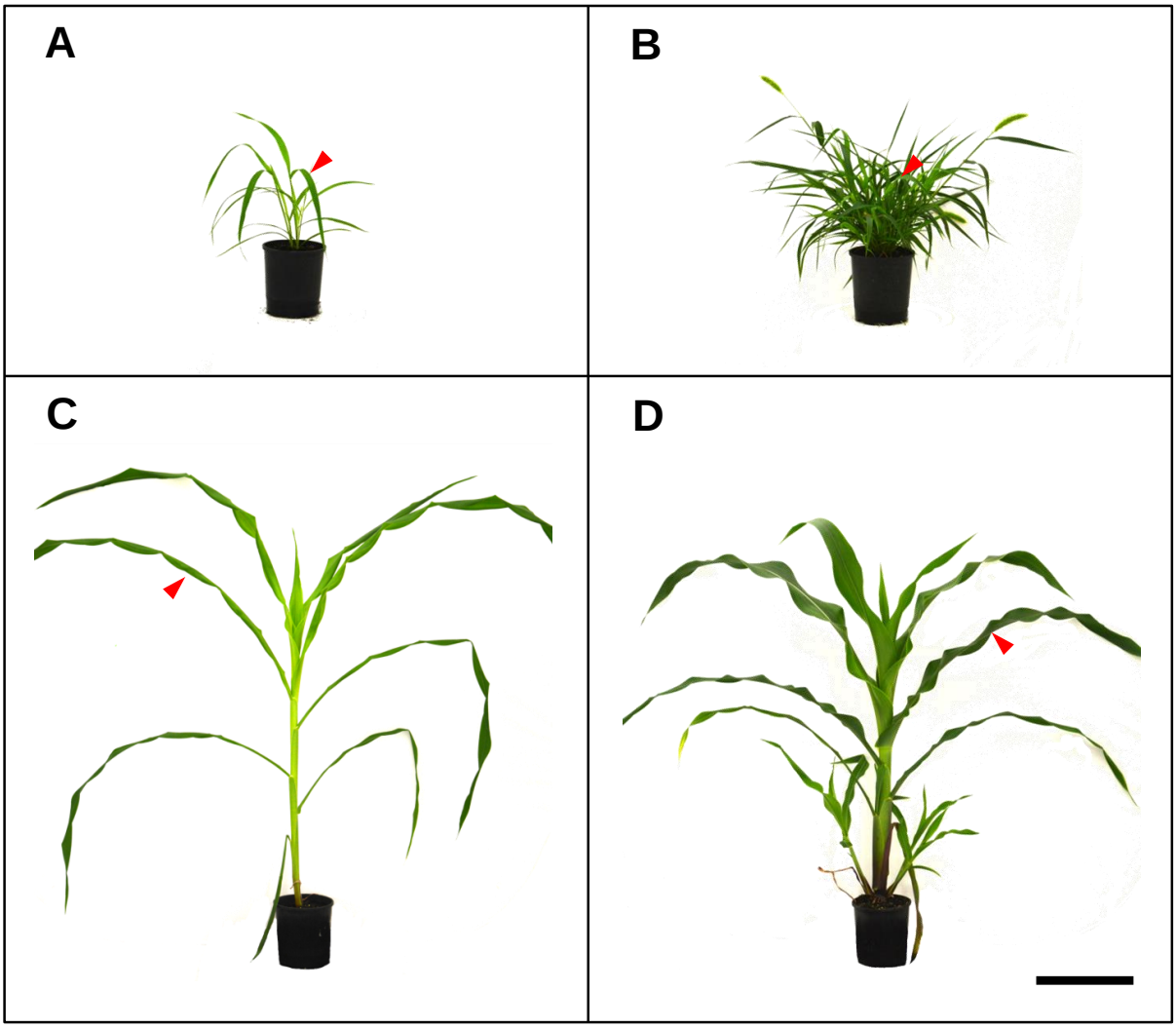

Supplementary Figure 2. Seven week-old *S. viridis* and *Z. mays* grown under different irradiances. Low light at 100 µmol m^{-2} s^{-1} and high light at 1000 µmol m^{-2} s^{-1}. (A) Low light-grown *S. viridis*, (B) high light-grown *S. viridis,* (C) low light-grown *Z. mays*, and (D) high light-grown *Z. mays*. Red arrowhead points to the leaf used for measurements and quantification. Bar = 20 cm.

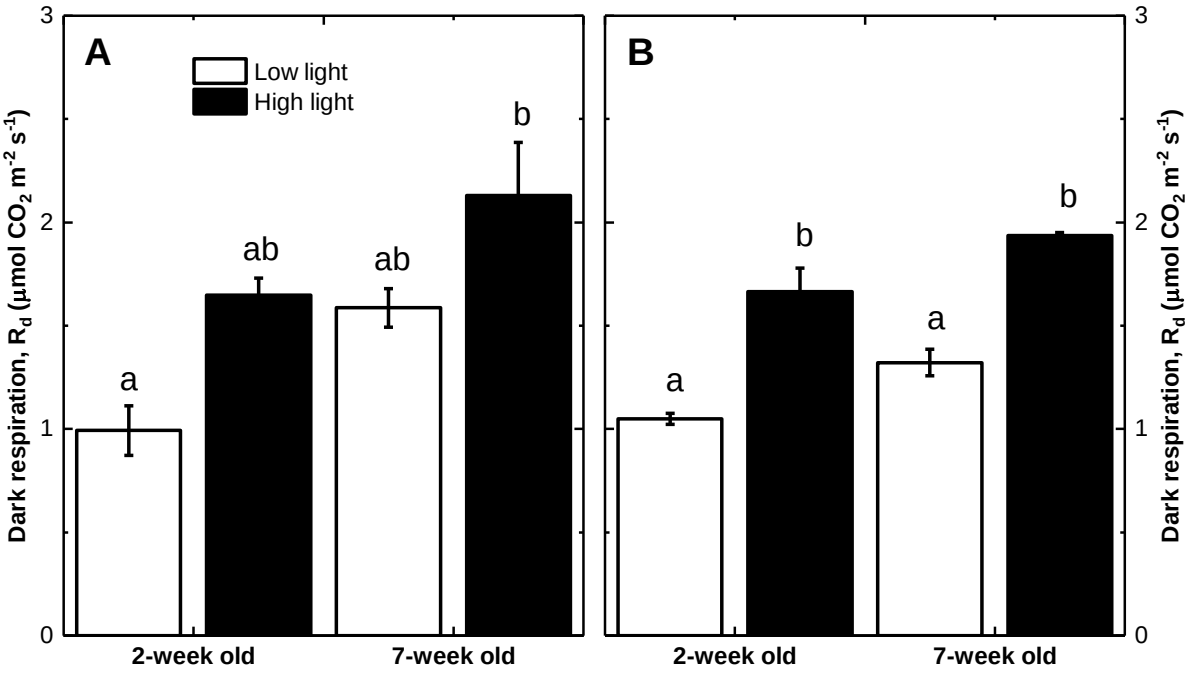

Supplementary Figure 3. Dark respiration rates of *S. viridis* (A) and *Z. mays* (B) grown under different growth irradiances. Each bar represents the mean ± SE, n=3. Letters indicate the ranking (lowest=a) using multiple-comparison Tukey's post-hoc test. Bars with same letter are not statistically different at $P<0.05$.